Implementing Conditional Hazard for Earthquake Engineering Practice: the Italian Example

E. Chioccarelli, S. Esposito & I. Iervolino
Università degli Studi di Napoli Federico II, Italy.

SUMMARY:
In the last years, among those for which seismic hazard is available, researchers have identified spectral acceleration $Sa(T_1)$ at the first mode period of the structure as one of the most convenient intensity measures (IM) for seismic analysis of engineering structures. However, there are cases in which alternative IMs have been found to be also important to complement the structural response information carried by $Sa(T_1)$. To account for them in a complementary manner, the concept of conditional hazard maps was introduced recently. It consists in maps of percentiles of a secondary IM given the occurrence or exceedance of a primary parameter, for which a design hazard map is already available (as it often happens for $Sa(T_1)$). In this paper, the conditional hazard concept is exploited further and maps, for some emerging IMs, are computed for the whole Italian territory. Results demonstrate how conditional hazard renders the use of vector-valued IMs easy and practice-ready, at the sole cost $Sa(T_1)$ is considered the primary IM, which in fact is the underlying hypothesis in several codes.

Keywords: Record selection, Vector-valued intensity measures, Disaggregation, Seismic Hazard.

1. INTRODUCTION

Accuracy of seismic analysis of engineering structures is strongly connected to the choice of a *good* (to follow) ground motion intensity measure (IM). In the last years, researchers have identified spectral acceleration at the first mode period of the structure, hereinafter $Sa(T_1)$, as one of the most convenient IMs. In fact, in many cases, for a given $Sa(T_1)$, the distribution of the engineering demand parameter (EDP) of interest is statistically independent from any other ground motion characteristics (i.e., it is *sufficient*) and shows a limited dispersion (i.e., it is *efficient*). Moreover, it is often possible to scale the all selected records to a fixed $Sa(T_1)$ value without introducing any systematic error (or bias) in the EDP estimation (i.e., it is *robust*) (Tothong and Luco, 2007).
Most importantly, use of such an IM was supported because classical probabilistic seismic hazard analysis (PSHA) (e.g., McGuire, 2004), and consequently more advanced international codes, quantifies the seismic threat in terms of probability of exceedance of this parameter.
At the same time, cases in which other IMs can be more appropriate, are known by literature. For example: (i) for structures with strong inelastic behavior, or sensitive to other modes than the first one, other portions of the elastic response spectrum may be important, and acceleration ordinates at other periods, or measures of the spectral shape in a range of periods can both be assumed as alternative IMs; (ii) integral IMs measuring duration or energy of ground motion may be relevant for structures with cycle-sensitive dynamic behavior (Cosenza and Manfredi, 2000). In fact, vector-valued IMs were considered (Bazzurro and Cornell, 2002) in order to account for more than one IM at the same time, yet complications derive from such a choice; e.g., the consequent need of computing vector-valued

PSHA.

To overcome the issues related to computing vector-valued hazard analysis, which is not only demanding, but also force to discard the marginal hazard available (for example that for $Sa(T_1)$), the concept of conditional hazard maps has been introduced recently (Iervolino et al., 2010a): it consists in maps of percentiles of a secondary IM (IM_2) given the occurrence or exceedance of a primary parameter (IM_1).

Some hypotheses are necessary for developing conditional hazard maps: (i) availability of ground motion prediction equations (GMPEs) for both IMs, (ii) availability of magnitude and distance hazard disaggregation distributions for the primary parameter, (iii) the joint normality[1] of the chosen IMs, and (iv) availability of their correlation coefficients. If these conditions are met, distribution of IM_2 conditional to IM_1 can be computed as in Eqn. 1.1 and Eqn. 1.2. These, according to most of GMPE models, are referred to (base 10) logarithm of IM_1 $(\log_{10} IM_1 = z)$ and $\log_{10} IM_2$, so that mean and standard deviation of the associated conditional normal distribution are represented by $\mu_{\log_{10} IM_2|\log_{10} IM_1}$ and $\sigma_{\log_{10} IM_2|\log_{10} IM_1}$ respectively.

$$\mu_{\log_{10}IM_2|\log_{10}IM_1} \approx \mu_{\log_{10}IM_2|\mathrm{M}^*,\mathrm{R}^*} + \rho_{\log_{10}IM_1,\log_{10}IM_2} \cdot \sigma_{\log_{10}IM_2} \frac{z - \mu_{\log_{10}IM_1|\mathrm{M}^*,\mathrm{R}^*}}{\sigma_{\log_{10}IM_1}} \tag{1.1}$$

$$\sigma_{\log_{10}IM_2|\log_{10}IM_1} = \sigma_{\log_{10}IM_2} \cdot \sqrt{1-\rho^2_{\log_{10}IM_1,\log_{10}IM_2}} \tag{1.2}$$

In Eqn. 1.1 $\{\mathrm{M}^*, \mathrm{R}^*\}$ is the vector of magnitude and distance indentifying *design earthquake* given the exceedance of hazard threshold of IM_1 (to be provided by disaggregation), $\rho_{\log_{10}IM_1,\log_{10}IM_2}$ is the correlation coefficient between logarithms of IM_1 and IM_2, $\sigma_{\log_{10}IM_1}$ and $\sigma_{\log_{10}IM_2}$ are the standard deviation of $\log_{10}IM_1$ and $\log_{10}IM_2$ provided by the corresponding GMPE and $\mu_{\log_{10}IM_1|\mathrm{M}^*,\mathrm{R}^*}$ and $\mu_{\log_{10}IM_2|\mathrm{M}^*,\mathrm{R}^*}$ are the expected values of $\log_{10}IM_1$ and $\log_{10}IM_2$ computed by the GMPE model given the occurrence of design earthquake.

In principle, left hand side of Eqn. 1.1 depends on the whole disaggregation distribution of M and R given the exceedance of $\log_{10}IM_1$. Above, the approximated form is reported in which such distribution is substituted by design earthquake. The latter can be identified, as an example, with modal values of disaggregation distribution (Iervolino et al., 2011). The approximation is as appropriate as disaggregation is dominated by a single magnitude and distance pair.

In the first application of conditional hazard (Iervolino et al., 2010a), discussed for sites within Campania region (southern Italy), chosen IMs were the spectral acceleration (primary) and the so-called Cosenza and Manfredi index, (I_D), a secondary parameter correlated to cumulated structural damage (Manfredi, 2001). Herein the conditional hazard concept is exploited further choosing three different secondary IMs complementing $Sa(T_1)$. Once all the information about specific implementation of conditional hazard are provided, maps of median values of conditional IMs are computed for the whole Italian territory. Moreover, some examples for specific sites are reported. Finally for one of the considered sites, an example of record selection accounting for design spectrum and conditional hazard (in terms of peak ground acceleration, PGV) is reported.

[1] This is not strictly necessary, as any joint distribution is suitable; nevertheless, if multi-normality assumption may be retained convenient analytical-form solutions follow.

2. SELECTING INTENSITY MEASURES

In this paper illustrative application of conditional hazard are reported considering different pairs of IMs. Primary IM is always spectral pseudo-acceleration at T_1 computed with a 5% damping ratio $Sa(T_1)$; IM_2 is chosen to carry information about the spectral shape at periods different from T_1. Thus, referring to a second period (T_2) of the same spectrum, selected IM_2 are: the ratio $(R_{T_1 T_2})$ between the two spectra accelerations (Eqn. 2.1), i.e. Cordova et al. (2001), and the ratio (Np) between geometric mean of spectral accelerations (Sa_{avg}) in the range of periods $[T_1, T_2]$ and $Sa(T_1)$ (Eqn. 2.2); i.e., Bojórquez and Iervolino (2011). For both of them, a value lower [higher] than one may indicate a negative [positive] slope of the response spectrum in the considered range of periods. However, Np may be more informative accounting for the spectral shape in a whole range rather than in the boundaries, yet at the cost of larger computational effort. T_1 and T_2 were assumed equal to 0.5 and 1 second, respectively.

$$R_{T_1 T_2} = Sa(T_2)/Sa(T_1) \tag{2.1}$$

$$Np = Sa_{avg}[T_1, T_2]/Sa(T_1) \tag{2.2}$$

Distributions of the logarithms of both $R_{T_1 T_2}$ and Np can be derived combining mean (μ) and variance (σ^2) of the logarithms of spectral ordinates (provided by the GMPE). Although specific analytical expressions are reported in the next sections, general rules for computation of these moments in case of linear combinations of random variables and constants are reported here. In particular being Y the random variable in Eqn. 2.3, its mean μ_Y and variance σ_Y^2 are reported in Eqn. 2.4 and Eqn. 2.5. $\{X_1, ..., X_n\}$ are also random variables, $\{a_1, ..., a_n\}$ are the combination coefficients, and $\rho_{i,j}$ is the correlation coefficient between X_i and X_j.

$$Y = \sum_i^n a_i \cdot X_i \tag{2.3}$$

$$\mu_Y = \sum_i^n a_i \cdot \mu_{X_i} \tag{2.4}$$

$$\sigma_Y^2 = \sum_{i=1}^n \sum_{j=1}^n a_i \cdot a_j \cdot \rho_{X_i, X_j} \cdot \sigma_{X_i} \cdot \sigma_{X_j} \tag{2.5}$$

It is worth nothing that, because $\log_{10}(R_{T_1 T_2})$ and $\log_{10}(Np)$ are linear combinations of logarithms of spectral periods, application of conditional hazard with such IM_2 provides similar information to those that can be derived using the conditional mean spectrum considering epsilon $(CMS - \varepsilon)$ introduced by Baker and Cornell (2006). On the other hand, advantages of conditional hazard is more evident if chosen IM_2 accounts for different ground motion characteristics with respect to response spectrum. In fact, it is presented a third illustrative application, in which selected IM_2 is the horizontal peak ground velocity (PGV).

The GMPE model provided by Bindi et al. (2011) was used referring to an Italian database of 765 ground motions from 103 events over the 4-6.9 moment magnitude range and characterized by source-to-site distance (i.e. the closest horizontal distance to the vertical projection of the rupture, the Joyner-Boore (1981) distance, R_{jb}) up to 196 km. Data distribution in terms of R_{jb}, M and soil type (according to Eurocode 8, CEN 2003) is reported in Figure 1.

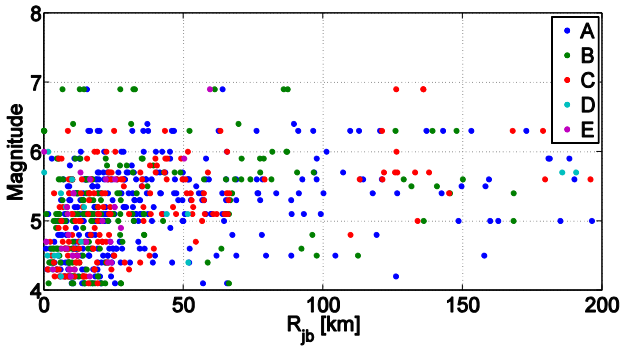

Figure 1 The strong-motion dataset with respect M, R_{jb} and local site conditions according to Eurocode 8 (CEN, 2003).

Correlation coefficients between the spectral periods in the $[T_1, T_2]$ interval were estimated using the same dataset of Bindi et al. (2011) through the Pearson product-moment estimator expressed in Eqn. 2.6 where *N* represents the number of records used for the estimation. Results are reported in Table 2.1, which is intended to be symmetrical.

$$\hat{\rho}_{\log_{10}(Sa(T_1)),\log_{10}(Sa(T_2))} = \frac{\sum_{i=1}^{N}\left(\log_{10}\left(Sa(T_1)\right)-\mu_{\log_{10}(Sa(T_1))}\right)\cdot\left(\log_{10}\left(Sa(T_2)\right)-\mu_{\log_{10}(Sa(T_2))}\right)}{\sqrt{\sum_{i=1}^{N}\left(\log_{10}\left(Sa(T_1)\right)-\mu_{\log_{10}(Sa(T_1))}\right)^2\cdot\sum_{i=1}^{N}\left(\log\left(Sa(T_2)\right)-\mu_{\log_{10}(Sa(T_2))}\right)^2}} \quad (2.6)$$

Table 2.1. Correlation coefficients for spectral ordinates between 0.5s and 1s period.

	T_2= 0.50s	**T_2= 0.60s**	**T_2= 0.70s**	**T_2= 0.80s**	**T_2= 0.90s**	**T_2= 1.00s**
T_1= 0.50s	1.00					
T_1= 0.60s	0.96	1.00				
T_1= 0.70s	0.92	0.97	1.00			
T_1= 0.80s	0.88	0.94	0.98	1.00		
T_1= 0.90s	0.86	0.91	0.95	0.98	1.00	
T_1= 1.00s	0.84	0.89	0.93	0.96	0.98	1.00

2.1. Ratio of pseudo-spectral acceleration as secondary intensity measure

In this case $R_{0.5,1} = Sa(1s)/Sa(0.5s)$ is chosen as IM_2. Although a GMPE for $\log_{10}\left(R_{0.5,1}\right)$ is not available, it can easily be derived as difference of normally distributed random variables. In fact normal distribution of $\log_{10} R_{0.5,1}$ follows from the normal distribution of $\log_{10} Sa(0.5s)$ and $\log_{10} Sa(1s)$; mean $\left(\mu_{\log_{10}R_{0.5,1}}\right)$ and variance $\left(\sigma^2_{\log_{10}R_{0.5,1}}\right)$ can be computed via Eqn. 2.7 respectively where $\mu_{\log_{10}Sa(0.5s)}$, $\mu_{\log_{10}Sa(1s)}$, $\sigma_{\log_{10}Sa(0.5s)}$ and $\sigma_{\log_{10}Sa(1s)}$ are provided by the original Bindi et al. (2011) GMPE model.

$$\begin{cases} \mu_{\log_{10}R_{0.5,1}} = \mu_{\log_{10}Sa(1s)} - \mu_{\log_{10}Sa(0.5s)} \\ \sigma^2_{\log_{10}R_{0.5,1}} = \sigma^2_{\log_{10}Sa(1s)} + \sigma^2_{\log_{10}Sa(0.5s)} - 2\cdot\rho_{\log_{10}Sa(0.5s),\log_{10}Sa(1s)}\cdot\sigma_{\log_{10}Sa(1s)}\cdot\sigma_{\log_{10}Sa(0.5s)} \end{cases} \quad (2.7)$$

The multivariate normality between the two IMs was tested via the skewness and kurtosis tests (Mardia, 1985) assuming a 0.99 significance level. Results are summarized in Table 2.2.
Correlation coefficient between $\log_{10} Sa(0.5s)$ and $\log_{10} R_{0.5,1}$ $\left(\rho_{\log_{10} Sa(0.5s),\log_{10} R_{0.5,1}}\right)$ was assessed to be equal to -0.23; see Eqn. 2.6.
It is worth noting that it can also be analytically derived knowing variance and covariance of $\log_{10} Sa(0.5s)$ and $\log_{10} Sa(1s)$. Results of two alternative procedures were checked to provide consistent results.

2.2. *Np* as secondary intensity measure

Similarly to the previous case, a GMPE for $\log_{10}(Np)$ can be derived as a combination of the lognormal distributions given by Bindi et al. (2011). In fact logarithmic analytical expression of Np is reported in Eqn. 2.8 where n is the number of periods between 0.5s and 1s in which pseudo-acceleration spectrum (Sa_i) can be computed by the considered GMPE model.

$$\log_{10} Np = \frac{1}{n} \cdot \sum_{i=1}^{n} \log_{10} Sa_i - \log_{10} Sa(0.5s) \tag{2.8}$$

Normality of the $\log_{10} Np$ distribution follows from normal distribution of each term on the right side of Eqn. 2.8. Mean predicted value of $\log_{10} Np$, $\mu_{\log_{10} Np}$, can easily be derived from the same equation, together with Eqn. 2.4, as reported in Eqn. 2.9:

$$\mu_{\log_{10} Np} = \frac{1}{n} \cdot \sum_{i=1}^{n} \mu_{\log_{10} Sa_i} - \mu_{\log_{10} Sa(0.5s)} \tag{2.9}$$

Recalling Eqn. 2.5, variance of the same distribution $\left(\sigma^2_{\log_{10} Np}\right)$ can be computed as shown in Eqn. 2.10. Similarly, variance of $\log_{10} Sa_{avg}$ can easily be derived and reported in Eqn. 2.11 :

$$\sigma^2_{\log_{10} Np} = \sigma^2_{\log_{10} Sa_{avg}} + \sigma^2_{\log_{10} Sa(0.5s)} - 2 \cdot \frac{1}{n} \cdot \sum_{i=1}^{n} \rho_{\log_{10} Sa_i,\log_{10} Sa(0.5s)} \cdot \sigma_{\log_{10} Sa_i} \cdot \sigma_{\log_{10} Sa(0.5s)} \tag{2.10}$$

$$\sigma^2_{\log_{10} Sa_{avg}} = \frac{1}{n^2} \cdot \sum_{i=1}^{n} \sum_{j=1}^{n} \rho_{\log_{10} Sa_i,\log_{10} Sa_j} \cdot \sigma_{\log_{10} Sa_i} \cdot \sigma_{\log_{10} Sa_j} \tag{2.11}$$

Numerical values of all correlation coefficients $\left(\rho_{\log_{10} Sa_i,\log_{10} Sa(0.5s)}\right)$ between 0.5s and 1s are those reported in Table 2.1. Joint normality between $\log_{10} Sa(0.5s)$ and $\log_{10} Np$ has been tested and results of the multivariate tests are reported in Table 2.2. Note that also in this case the multivariate skewness and kurtosis are not significant at the 0.99 significance level.
For the numerical implementation of Eqn. 1.1 and Eqn. 1.2, ρ value between $\log_{10} Sa(0.5s)$ and $\log_{10} Np$ is also necessary: it was assessed to be equal to -0.21.

2.3. *PGV* as secondary intensity measure

In this case, independent distributions of both intensity measures are provided by the same GMPE model, along with statistics. The multivariate normality assumption were tested and results in terms of p-value are reported in Table 2.2. Correlation coefficient $\left(\rho_{\log_{10} Sa(0.5s),\log_{10} PGV}\right)$ was assessed by the authors to be equal to 0.88.

Table 2.2. Test for joint normality for different secondary intensity measures.

	P-values		
	$R_{0.5,1}$	*Np*	*PGV*
Test of Swekness	0.0375	0.0371	0.0122
Test of Kurtosis	0.4826	0.5165	0.0103

3. APPLICATIONS

In this section examples of numerical implementation of conditional hazard are presented. First, considering the whole Italian region, the map of $Sa(0.5s)$ hazard for 457 yr Tr is shown in Figure 2a: it is computed on a grid of about 10,760 points using the same specifically developed software of Iervolino et al. (2011) to which the reader is referred for further details. Seismogenic sources are those of Meletti et al (2008) while seismic parameters of each zones are those from Barani et al. (2009 and 2010).

Hazard disaggregation was computed for $Sa(0.5s)$ using the same software and first-mode values of moment magnitude and epicentral distance distributions (used as design earthquakes) are reported in Figure 2b and Figure 2c. Finally in Figure 2d,e,f, maps of fiftieth percentile of conditional distribution of each considered IM_2 are reported for $R_{0.5,1}$, Np and PGV, respectively. It is to underline here that both hazard for $Sa(0.5s)$ and its disaggregation (in terms of modal values), are the necessary information common to all the conditional hazard maps: i.e., z and $\{M^*,R^*\}$ terms in Eqn. 1.1.

3.1 Site-specific applications

Choosing the specific site of S. Angelo dei Lombardi (latitude: 40.89°, longitude: 15.18) in southern Italy, conditional hazard distributions can be analyzed, and the influence of considered return period (Tr) can be discussed. In particular return periods equal to 475 and 2475 year were selected. Disaggregation distributions at 0.5s are reported in Figure 3a and Figure 3b respectively in which geographical site location and seismogenic zones contributing to hazard of the site, are also represented. Identifying design earthquakes as the modal value of disaggregation distribution (i.e., Iervolino et al., 2011), it appears that, for the considered spectral period, a single design earthquake exists for each Tr (Table 3.1).

Being hazard for the site dominated by a single seismogenic source, the one in which this site is enclosed into (Iervolino et al., 2011), differences between design earthquakes for different Tr are significant only referring to magnitude values.

Figure 3c shows the distribution of $R_{T_1 T_2}$ and Np conditional to $Sa(0.5s)$ hazard in terms of complementary cumulative distribution function. Influence of Tr is apparent, and predicted conditional values increase with the increasing of Tr. Similarly, conditional distributions of PGV, for the same site and return periods, are reported in Figure 3d.

Table 3.1. Design earthquakes for S. Angelo dei Lombardi.

Tr= 475		Tr= 2475	
M*	R*	M*	R*
6.13	6.5	6.88	6.5

As mentioned previously, approximation of Eqn. 1.1 is expected to be significant if disaggregation distribution is not dominated by a single value of $\{M, R\}$ vector. This may be the case of two different seismogenic zones contributing to the hazard at the site, causing a bimodal disaggregation distribution. In this condition it is possible to calculate two different distributions of conditional hazard, considering as design earthquakes first and second modal values of disaggregation, alternatively.

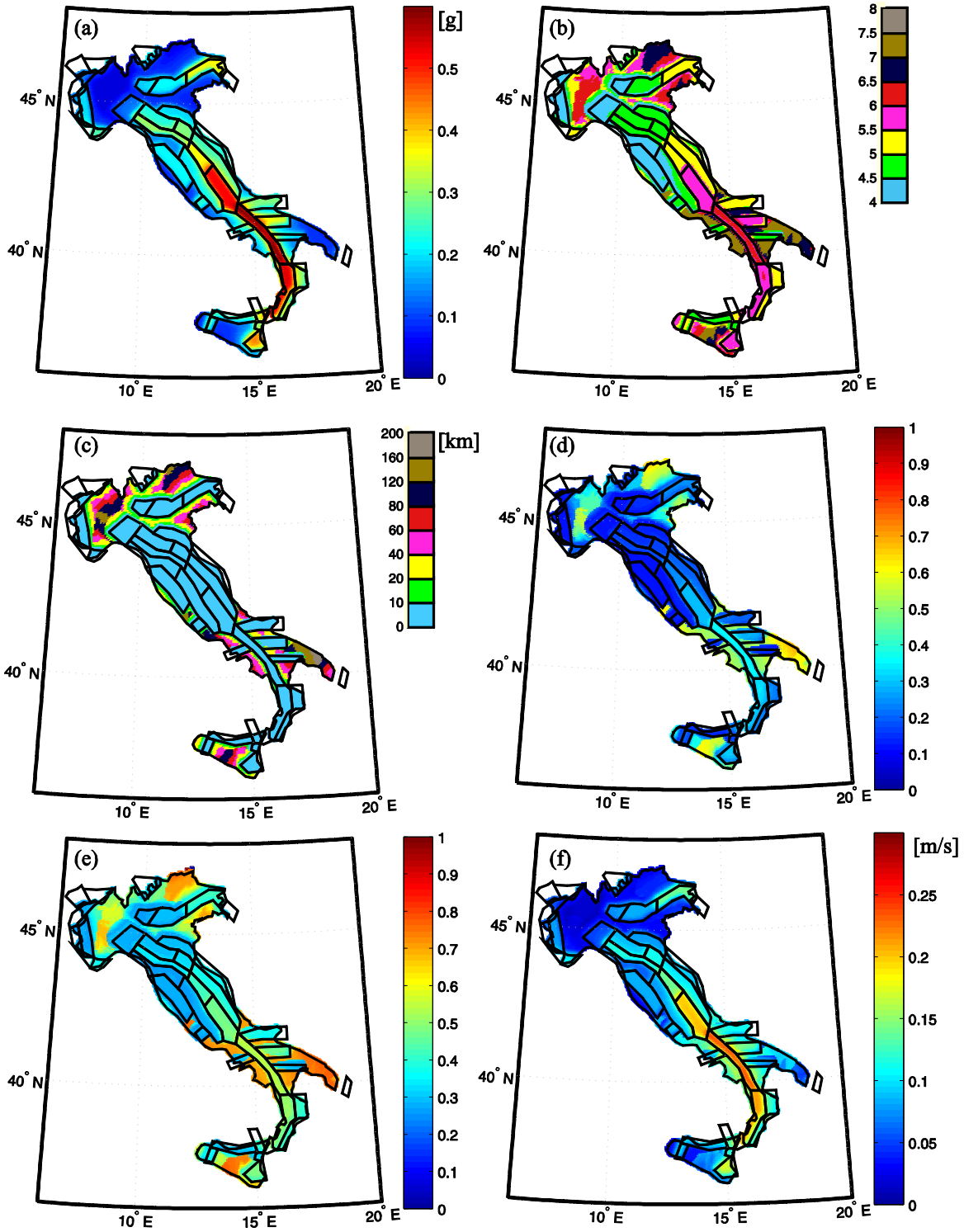

Figure 2. Map of Tr=475yr seismic hazard at 0.5s (a) and first-mode values of its disaggregation distribution in terms of moment magnitude (b) and epicentral distance (c); median values of conditional hazard for R_{T1T2} (d), Np (e) and PGV (f).

Another illustrative example is here reported for the site of Terni (latitude: 42.3°, longitude: 12.4°) whose disaggregation distribution at $0.5s$ and Tr=475yr (shown in Figure 4a) identifies two design earthquakes equal to $\{4.3, 5.5\}$ and $\{7.1, 60.5\}$ in terms of magnitude and distance. Figure 4a also shows hazard distributions of PGV conditional to $\mathrm{Sa}(0.5\mathrm{s})$ and referring to 1st and 2nd modal values. Same comparisons are reported in Figure 4b for the shape-related IM_2. Sensitivity to chosen design

earthquakes is apparent. Specifically for the analyzed site, $\{M^*, R^*\}$ pairs associated with the second mode, causes median value of IM_2 $\left(\mu_{\log_{10} IM_2|M^*,R^*}\right)$ higher than that associated to the first mode.

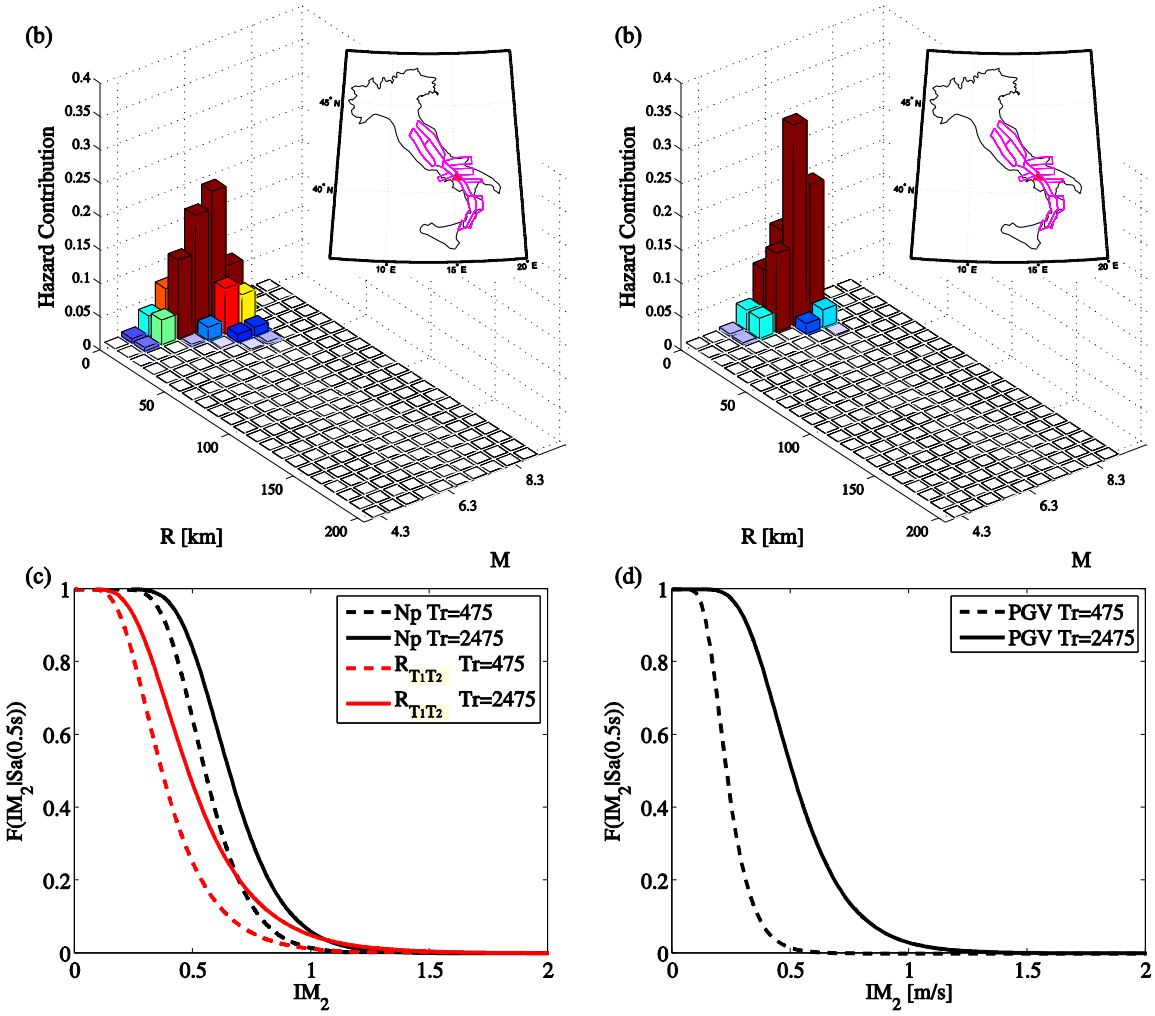

Figure 3. Disaggregation distribution for S. Angelo dei Lombardi and two different return period: 475 yr (a) and 2475yr (b); Conditional distribution of R_{T1T2} and Np (c) and PGV (d) for the same site

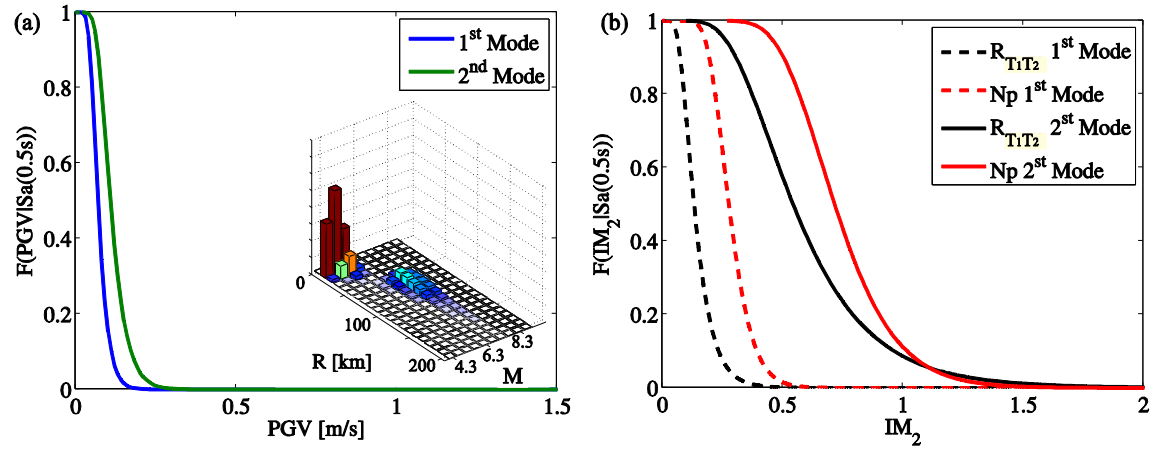

Figure 4. Disaggregation distribution and conditional hazard of PGV (a), R_{T1T2} and Np (b) considering first and second design earthquake for Terni and Tr=475yr.

3.2 Example of practice-related use of conditional hazard

As mentioned conditional hazard is a ready tool for record selection in earthquake engineering practice. In order to demonstrate it, a selection of two set of records for the site of Terni is provided. Used software is REXEL (available at http://www.reluis.it/index.php?lang=en), which searches for suites of waveforms compatible on average to various types of code-based or user defined spectra (Iervolino et al., 2010b). Hazard at the site was identified by the design spectrum from Italian code (CS.LL.PP, 2008) with site class A (according to CEN, 2003) and Tr = 475yr. Chosen range of periods in which REXEL warrants spectral compatibility is $[0.5\text{s}, 2\text{s}]$, that is, average of selected record set (of seven) is higher than the 90% and lower than 130% of design spectrum.
The software also allows to constrain selection referring to additional IMs. In this case, recalling that median values of conditional PGV distribution in Figure 4a are equal to 0.07 m/s and 0.11 m/s referring to first or second modal value of disaggregation distribution respectively, ranges of PGV were chosen as $[0.05, 0.09]$ m/s and $[0.08, 0.14]$ m/s. Found spectrum-compatible sets are reported in Figure 5a and b, and show a mean PGV different, being equal to 0.07 m/s and 0.11 m/s, respectively. On the other hand sets can be considered equivalent with respect to spectral compatibility in the selected range of periods.

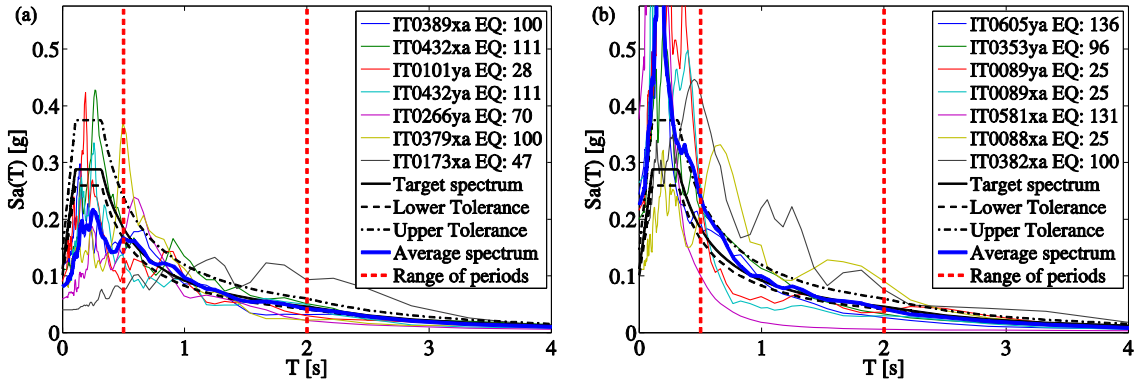

Figure 5. Record selection for Terni and Tr=475yr considering spectrum compatibility and PGV values derived from 1st and 2nd modal values of disaggregation.

3. CONCLUSIONS

In the presented study the concept of conditional hazard was explored showing illustrative applications for the Italian territory. Three different pairs of primary and secondary intensity measures were chosen. Maintaining $\text{Sa}(0.5\text{s})$ as primary, $R_{T_1 T_2}$, Np and PGV were alternatively selected as secondary IMs. Correlation coefficients between chosen intensity measures were estimated on the same Italian ground motion database to which the used GMPE refers. Normality of joint distributions was also checked for each pair of IMs. Required design earthquakes were selected as the modal values of magnitude and distance disaggregation distributions.
Such data, allowed to computed maps of median values of secondary intensity measure conditional to the exceedance of the primary. Illustrative examples refer to maps for a return period equal to 475 years.
Site-specific applications were also shown. For the site of S. Angelo dei Lombardi, examples of conditional distributions were reported underlining the influence of return period. The site of Terni was also considered: being the hazard influenced by two different seismogenic zones, its disaggregation distribution is dominated by two different design earthquakes. In this condition, it is shown that two different conditional hazard distributions should be. Finally, an example of record selection for the same site is provided in order to demonstrate that conditional hazard is a practice-ready tool for record selection for earthquake engineering applications.

ACKNOWLEDGMENT

This research was developed in the framework of *AMRA – Analisi e Monitoraggio dei Rischi Ambientali scarl* (http://www.amracenter.com). The results shown were developed within the *Strategies and tools forReal-Time Earthquake Risk Reduction* (REAKT;http://www.reaktproject.eu) projects. It is funded by the European Community via the *Seventh Framework Program for Research* (FP7),with contract no.282862. Authors want to thank Dr. Dino Bindi (*Deutsches GeoForschungsZentrum*, Germany) and Dr. Francesca Pacor (*Istituto Nazionale di Geofisica e Vulcanologia*, Italy), for kindly providing us with datasets used in this study.

REFERENCES

Baker, J. and Cornell, N. (2006). Spectral shape, epsilon and record selection. *Earthquake Engineering and Structural Dynamics*, **35**, 1077-1095.

Barani, S., Spallarossa, D., Bazzurro, P. (2009). Disaggregation of probabilistic ground motion hazard in Italy. *Bulletin of Seismological Society of America* **99:5**, 2638-2661.

Barani, S., Spallarossa, D., Bazzurro, P. (2010). Erratum to disaggregation of probabilistic ground motion hazard in Italy. *Bulletin of Seismological Society of America* **100:6**, 3335-3336.

Bazzurro, P., and Cornell, C. A. (2002). Vector-valued probabilistic seismic hazard analysis. *7th U.S. National Conference on Earthquake Engineering*, Boston, MA, 10 pp.

Bindi, D., Pacor, F., Luzi, L., Puglia, R., Massa, M., Ameri, A. and Paolucci, R. (2011). Ground motion prediction equation from the Italian strong motion database. *Bulletin of Earthquake Engineering*, **31,** 1899-1920.

Bojórquez, E. and Iervolino,I., (2011). Spectral shape proxies and nonlinear structural response. *Soil Dynamics and Earthquake Engineering*, **31:7**, 996-1008.

CEN, European Committee for Standardization TC250/SC8/(2003) Eurocode 8: Design provisions for earthquake resistance of structures. *Part 1.1: general rules, seismic actions and rules for buildings*, PrEN1998-1.

Cordova, P. P., Dierlein, G. G., Mehanny, S. S. F. and Cornell C. A. (2001) Development of a two parameter seismic intensity measure and probabilistic assessment proce- dure. S*econd U.S.–Japan workshop on performance- based earthquake engineering methodology for reinforce concrete building structures*. p. 187–206.

Cosenza, E. and Manfredi, G. (2000). Damage indices and damage measueres. *Progress in Structural Engineering and Materials*, **2**, 50-59.

CS.LL.PP. DM 14 gennaio 2008 Norme Tecniche per le Costruzioni. *Gazzetta Ufficiale della Repubblica Italiana*, **29** [in Italian].

Iervolino I., Galasso C. and Cosenza E. (2010b). REXEL: computer aided record selection for code-based seismic structural analysis. *Bulletin of Earthquake Engineering*, **8**, 339–362.

Iervolino, I., Chioccarelli, E. and Convertito, V. (2011). Engineering desegn earthquakes from multimodal hazard disaggregation. *Soil Dynamics and Earthquake Egineering.* **31**, 1212-1231.

Iervolino, I., Giorgio, M., Galasso, C. and Manfredi, G. (2010a). Conditional hazard maps for secondary intensity measures. *Bulletin of Seismological Society of America.* **100:6**, 3312-3319.

Joyner, W.B. and Boore, D. M. (1981). Peak horizontal acceleration and velocity from strongmotion records including records from the 1979 Imperial Valley, California, Earthquake. *Bulletin of the Seismological Society of America* **71**, 2011–38.

Manfredi, G.(2001). Evaluation of seismic energy demand. *Earthquake Engineering and Structural Dynamics* **30**, 485–499.

Mardia, K. V. (1985). Mardia's test of multinormality. *Encyclopedia of Statistical Sciences*, S. Kotz and N. L. Johnson (Editors), **5**, 217–221.

McGuire, R. K. (2004) Seismic Hazard and Risk Analysis. *Earthquake Engineering Research Institute*, MNO-10, Oakland, California, 178 pp.

Meletti, C., Galadini, F., Valensise, G., Stucchi, M., Basili, R., Barba, S., Vannucci, G. and Boschi, E. (2008). A seismic source zone model for the seismic hazard assessment of the italian territory. *Tectonophysics* **450**, 85–108.

Tothong, P. and Luco, N. (2007). Probabilistic seismic demand analysis using advaced ground motion intensity measures. *Earthquake Engineering and Structural Dynamics* **36**, 1837-1860.